



UNIVERSITY OF LEEDS

This is a repository copy of *Evaluation of laboratory techniques for assessing scale inhibition efficiency*.

White Rose Research Online URL for this paper:
<http://eprints.whiterose.ac.uk/149698/>

Version: Accepted Version

Article:

Sanni, OS, Bukuaghangin, O, Charpentier, TVJ orcid.org/0000-0002-3433-3511 et al. (1 more author) (2019) Evaluation of laboratory techniques for assessing scale inhibition efficiency. *Journal of Petroleum Science and Engineering*, 182. 106347. ISSN 0920-4105

<https://doi.org/10.1016/j.petrol.2019.106347>

© 2019 Elsevier B.V. All rights reserved. Licensed under the Creative Commons Attribution-Non Commercial No Derivatives 4.0 International License (<https://creativecommons.org/licenses/by-nc-nd/4.0/>).

Reuse

This article is distributed under the terms of the Creative Commons Attribution-NonCommercial-NoDerivs (CC BY-NC-ND) licence. This licence only allows you to download this work and share it with others as long as you credit the authors, but you can't change the article in any way or use it commercially. More information and the full terms of the licence here: <https://creativecommons.org/licenses/>

Takedown

If you consider content in White Rose Research Online to be in breach of UK law, please notify us by emailing eprints@whiterose.ac.uk including the URL of the record and the reason for the withdrawal request.



eprints@whiterose.ac.uk
<https://eprints.whiterose.ac.uk/>

Evaluation of laboratory techniques for assessing scale inhibition efficiency

Olujide S. Sanni^{†*}, Ogbemi Bukuaghangin[†], Thibaut V. J. Charpentier^{††}, Anne Neville[†]

[†]School of Mechanical Engineering, University of Leeds, UK

^{††}School of Chemical and Process Engineering, University of Leeds, UK

*Corresponding author: o.s.sanni@leeds.ac.uk.

Abstract

Injecting chemical inhibitors is the most common method to mitigate mineral scaling in the oil industry. As such, the effectiveness of the techniques employed to evaluate performance of chemical scale inhibitors and apply the appropriate dosage is a very important aspect to be considered during the design of a scale prevention treatment. In this paper, the kinetics of scale formation and its inhibition are studied using a conventional bottle test, a dynamic tube blocking rig and a recently developed in-situ flow visualization rig. Calcium carbonate scaling brine was prepared at two saturation indices (SI) of 2.1 and 2.8 at 50°C and run through the rigs at flow rate of 20ml/min. The conventional polphosphinocarboxylic acid (PPCA) inhibitor was used for the inhibition study at concentration ranging between 0.5–10ppm. The MIC_{bulk} determined from bottle test and supported with the in-situ turbidity MIC_{bulk} for SI of 2.1 and 2.8 are 1ppm and 8ppm respectively. For the same SI values, a considerably lower concentration of PPCA, 0.5ppm and 4ppm for the surface inhibition test using the capillary rig were obtained compared to MIC_{surface} of 4ppm and 8ppm from the in-situ visualization technique. The surface visualization technique enables the range of concentration of inhibitors at which both bulk and surface scaling are completely controlled to be determined. The different techniques are shown to give complementary information for different stages of crystallization process and inhibition.

Keywords: Scaling; CaCO₃; Techniques; Crystal growth; Inhibition

1 Introduction

The performance and efficiency of chemical scale inhibitors to prevent mineral scaling in bulk solutions and on surfaces of equipment in the oilfield industry cannot be compromised. Great attention has been given to inhibition of bulk precipitation reactions (Amjad, 1994; Boak et al., 1999; Shaw and Sorbie, 2013; Shaw, 2012; Tomson et al., 2005).

40 The conventional bottle tests used for evaluating the efficiency of scale inhibitor
41 usually focus on the inhibition of bulk scale precipitation processes. Bulk jar test
42 consists of mixing brine in a beaker or a jar and carrying out an assessment of the
43 precipitation process (Graham et al., 2005). At the range of temperature (5°C, 50°C
44 and 95°C) usually encountered in the production system, it was demonstrated that the
45 dosage of inhibitor marginally below the required minimum concentration can actually
46 enhance surface scale growth (Graham et al., 2005; Morizot, 1999a).

47
48 Dynamic tube-blocking rigs have been widely used for the study of scaling phenomena
49 and in particular for the ranking of scale inhibitors (Dyer and Graham, 2002; Liu et al.,
50 2012; Liu et al., 2016). A typical tube blocking rig experiment involves measurements
51 of the differential pressure across a small diameter bore tubing of approximately 1-2m
52 length (Bazin et al., 2005; Bazin et al., 2004; Dyer and Graham, 2002). The time for
53 the pressure across the cell to increase and deviate from the baseline value gives a
54 measure of the scaling time. Such technique is often used to assess the efficiency of
55 scale inhibitors before being deployed in the production lines. Tube blocking tests were
56 used by Zhang et al (Zhang et al., 2001) to perform bulk measurements at the outlet
57 of the tube and to develop a kinetic model to predict downhole scaling. Dyer and
58 Graham (Dyer and Graham, 2002) studied the effects of temperature and pressure on
59 barium sulphate and calcium carbonate precipitation. The relative efficiency of two
60 inhibitors combined with temperature and pressure effects on scale formation was also
61 assessed using the dynamic tube blocking rig with good success. Inhibitor efficiency
62 is measured by the ratio of the time needed to block the tube in the presence of
63 inhibitor divided by the time needed to block the tube without inhibitor (Bazin et al.,
64 2004). The drawback of this technique is that the reduction of ionic species as scale
65 is formed in the 1-2m long tubing coil with residence time of above 3s at 20ml/min, will
66 cause a decrease in the saturation ratio and possibly uneven distribution of deposited
67 scale along the tubing. It is therefore difficult to use the methodology to develop a
68 robust kinetic models where the experimental conditions should remain constant
69 across the working section. The possibility of scale gradually building up in the
70 capillary or tube without effectively detecting it could also lead to incorrect assessment
71 of the Minimum Inhibitor Concentration (MIC).

72
73 An in-situ flow visualization technique with associated image analysis of scale build-
74 up in real-time was recently developed to study the kinetics and mechanisms of
75 surface scaling under constant condition (Sanni et al., 2015; Sanni et al., 2017). It was
76 used to assess the inhibition of BaSO₄ surface and bulk scaling using phosphino-
77 polycarboxylic acid (PPCA) and di-ethylene triamine penta methylene phosphonic acid
78 (DETPMP) (Bukuaghangin et al., 2016). Scale precipitation and surface deposition is
79 followed in-situ and in real-time in a once-through flow rig that allows control and
80 assessment of various parameters such as temperature, flow rate, inhibitor
81 concentration, brine chemistry and scaling indices. Having a constant supersaturation
82 across the working section is important to be able to accurately predict scaling kinetics
83 and effectively evaluate the MIC.

84

85 Recent studies are now being focussed on the evaluation and inhibition of surface
86 fouling and crystal growth rates at solid interfaces (Bukuaghangin et al., 2016;
87 Charpentier et al., 2015; Keogh et al., 2017). Chen et al (Chen, 2005) reported that at
88 4 ppm of PPCA, the inhibition efficiency of surface deposition is greater than the
89 inhibition efficiency of bulk precipitation. It is assumed that the inhibitor film formed on
90 the metal surface at the highest concentration of PPCA (4 ppm) prevent the adsorption
91 of scale crystals on the metal surface. Other studies have shown that the mechanisms
92 and kinetics controlling bulk and surface deposition are different and scale inhibition
93 efficiency varies between surface and bulk processes (Chen et al., 2005; Mavredaki,
94 2009; Morizot and Neville, 2000; Sanni et al., 2015; Setta and Neville, 2011).

95

96 As such, there is need to evaluate existing bulk inhibition methods and establish their
97 suitability to assess surface inhibition by focussing on the distinction between bulk and
98 surface mechanisms and the effects on inhibition strategies. The current paper,
99 therefore assesses and compares the inhibition performance of PPCA using the
100 conventional bottle, dynamic tube blocking rig, a new capillary system as well as the
101 newly developed once-through in-situ flow visualization technique. The new technique
102 has been used at the same condition as the conventional methods in order to
103 simultaneously and distinctively study the inhibition of both homogeneous bulk
104 precipitation and heterogeneous surface deposition in a single system. The results are
105 further analysed to show effects of chemical inhibition on crystallization mechanisms
106 using a model developed by Beaunier et al (Beaunier et al., 2001) and subsequently
107 modified by Euvrard et al (Euvrard et al., 2006). It describes the types of nucleation as
108 either instantaneous or progressive. Instantaneous nucleation describes the situation
109 when, in the initial stages of crystal formation, nuclei are formed and then grow. The
110 nucleation and growth processes are separated, and no further nucleation occurs
111 when the growth is occurring while progressive nucleation describes the process when
112 nucleation occurs and the crystals grow but new nuclei continue to be formed.

113

114 For instantaneous nucleation:

$$S_{ext}(t) = -\ln(1 - S(t)) = \frac{MK_1N_0t}{\rho} \quad (1)$$

115

116 For Progressive nucleation:

$$S_{ext}(t) = -\ln(1 - S(t)) = \frac{MK_1N_0At^2}{\rho} \quad (2)$$

117 $S_{ext}(t)$ is the extended surface coverage, $S(t)$ is the actual covered surface area, A is
118 the nucleation rate, k_1 is the lateral growth rate (mol/ $\mu\text{m}/\text{s}$), M is the molar mass of
119 CaCO_3 (100g/mol), ρ is the density of the crystals ($\rho=2.71 \times 10^{-12}\text{g}/\mu\text{m}^3$ for calcite),
120 N_0 is the number of active nucleation sites (equivalent to detected number of crystals).

121 Instantaneous nucleation occurs when $S_{ext}(t)$ is proportional to time, whereas
 122 progressive nucleation takes place when $S_{ext}(t)$ is proportional to time squared (t^2).
 123

124 2 Experimental Details

125 2.1 Chemical

126 2.1.1 Brine Composition

127 Two brines were mixed at 50:50 at a temperature of 50°C and at atmospheric pressure.
 128 The saturation ratio of these brines was calculated using the ScaleSoftPitzer (Version
 129 4.0) (Tomson, 2009). Saturation ratio is calculated generally using equation (3).

$$SR = \frac{[Ca^{2+}][CO_3^{2-}]}{K_{spCaCO_3}} \quad (3)$$

130 The composition of the brines used is presented in Table 1 and Table 2. The seawater
 131 (SW) is the source of carbonate ions (CO_3^{2-}) while the Formation Water (FW) is the
 132 source of calcium ions (Ca^{2+}) in the experiment. Each brine shows a simple
 133 composition to prevent the influence of impurities on the formation of $CaCO_3$ scale.

134 The scaling tendency can also be expressed in terms of Saturation Index (SI), which
 135 is the logarithm of Saturation Ratio (SR)

$$SI = \log_{10} SR \quad (4)$$

136

137

Table 1: Brine Composition in g/l for SI 2.1

	NaCl	NaHCO₃	CaCl₂.2H₂O
Formation water	46.36	0	7.35
Sea water	31.02	5.51	0
Supersaturation index SI (50:50)	2.1 (SR = 126)		

138

139

Table 2: Brine Composition in g/l for SI 2.8

	NaCl	NaHCO₃	CaCl₂.2H₂O
Formation water	46.36	0	14.70
Sea water	31.02	11.70	0
Supersaturation index SI (50:50)	2.8 (SR = 630)		

140

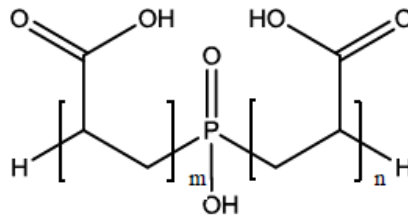
141 The two concentrations were selected to induce both homogeneous bulk and
 142 heterogeneous surface precipitation within a reasonable time frame. The temperature

143 of 50°C selected was based on temperature observed in an oilfield topside
144 operations(Graham et al., 2005).

145 2.1.2 Additives

146 The chemical additive used during the study is PPCA, which is a commercial product
147 commonly used in the oilfield because of its good quality, low cost and environmental
148 acceptability. PPCA is a standard polymeric scale inhibitors widely applied in the field
149 to prevent both carbonate and sulphate scales (Farooqui et al., 2014)

150 The molecular weight of PPCA IS 3600g/mol and its molecular structure shown in
151 Figure 1.



152

153

Figure 1: Schematic structures of PPCA (Amjad, 1998)

154 2.1.3 Cleaning solution

155 In order to reduce error and increase good reproducibility, the rigs were cleaned up
156 after each experiment with a solution containing 25g of ethylene-diamine-tetra-acetic
157 acid (EDTA) and 25g of potassium hydroxide (KOH) in 500 ml (pH of ~11).

158 2.2 Experimental Set-up

159 2.2.1 Bulk Jar/Bottle Test

160 This is the common test method used to evaluate the efficiency of chemical scale
161 inhibitors in bulk solution. The test procedures for the conventional bottle test
162 performed are as described in the NACE standards (NACE, 2001). The experiment
163 involves the mixing of brine in a beaker/jar the precipitation is then followed by
164 measuring the concentration of free calcium ions in solutions over time (t). The
165 efficiency of the inhibitor is calculated by using the equation:

$$I.E = 100 \left[\frac{C(t) - C_b(t)}{C_0 - C_b(t)} \right] \quad (5)$$

166

167 Where C (t) = test sample Ca²⁺ concentration at time, t, C_b(t) = Ca²⁺ concentration in
168 the blank solution (no scale inhibitor) and C₀ = control sample Ca²⁺ concentration at
169 time, t = 0 (ppm).

170 CaCO₃ brine solutions at SI values of 2.1 and 2.8 are prepared separately and tested.
171 PPCA inhibitors at different concentrations ranging from 1ppm – 10ppm were added
172 to each solution and the solutions were incubated at 50°C for 2 and 22 hours.

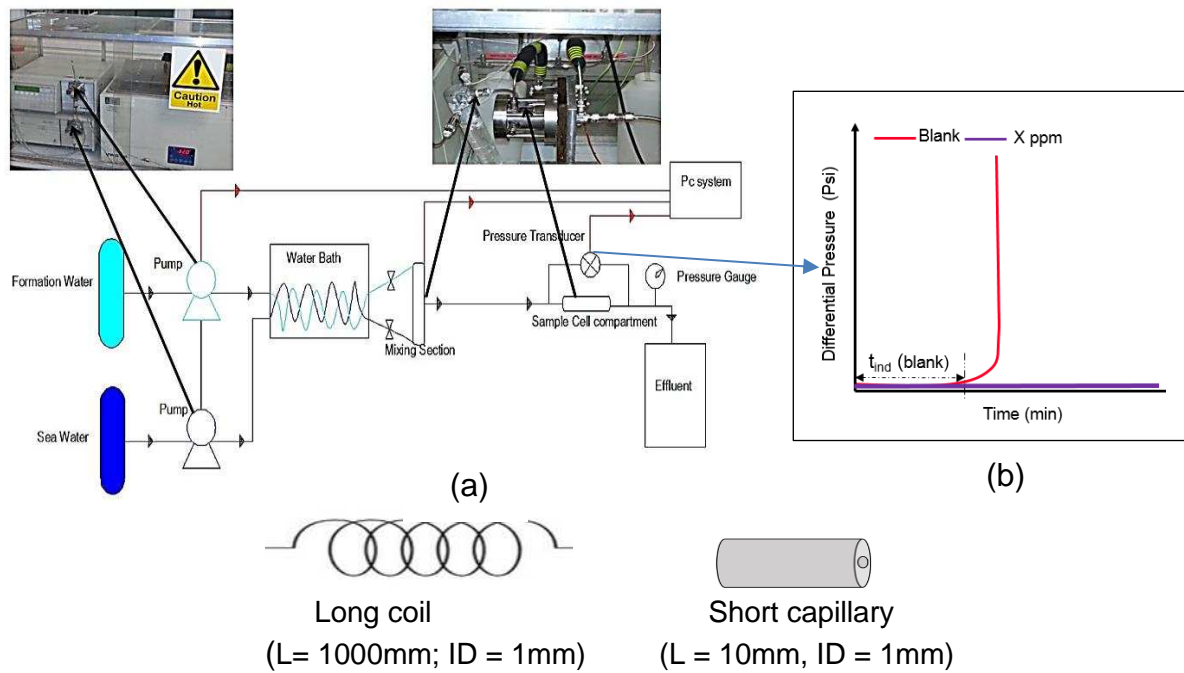
173 Uninhibited CaCO₃ brine serves as baseline conditions. After incubation, 1 ml sample
174 is taken from each bottle for chemical analysis using the Atomic Absorption
175 Spectrometry (AAS) analysis to determine the free calcium ion concentration
176 remaining in solution. 9 ml of a quenching (KCl/polyvinyl sulfonate) solution is added
177 to each sample to prevent further precipitation. The concentration of gas-phase atoms
178 is measured by the AAS using light absorption (Seeger et al., 2019). The analyte
179 atoms or ions is vaporized in a flame or graphite furnace. The light source is a hollow
180 cathode lamp in which the cathode is made from the same metal that is being
181 analysed, in this case calcium. The calcium atoms are excited on heating and their
182 electrons go to higher energy levels. When the electrons fall back to lower levels,
183 visible radiation is given off. The energy of the emitted photons corresponds to the
184 energy difference of the Ca atom electron levels. Concentration measurements are
185 usually determined from a working curve after calibrating the instrument with
186 standards of known concentration. Calcium ion standard solution of 1.0 mg ml⁻¹, was
187 prepared by dissolving an appropriate amount of CaO in diluted hydrochloric acid.

188 2.2.2 Capillary flow rig

189 The dynamic tube blocking test is a well-known technique used in the oil and gas
190 industry to investigate the effectiveness of scale inhibitor in dynamic conditions (Dyer
191 and Graham, 2002; Frenier, 2008; Graham et al., 2005). The set-up is equipped with
192 a temperature controlled device and a pressure transducer which is used to measure
193 the pressure difference across the tube as illustrated in the schematic diagram shown
194 in Figure 2. The brine solutions (SW and FW) are injected into the coils using a
195 reciprocating pump. The residence time of the fluid to travel from the mixing section to
196 the cells is 0.54s at flow rate of 20ml/min. Supersaturated solutions flow through a thin
197 tube of 1mm in diameter and scale builds up on the surface of the tube results in
198 differential pressure between the inlet and outlet of the tube (Frenier, 2008;
199 Koutsoukos and Kontoyannis, 1984) . In this study, two capillary tubes with lengths of
200 10mm and 1000mm (both internal diameters of 1mm) were used during the
201 experiment. The short capillary tube is the adapted version of the conventional tube
202 blocking rig where the saturation ratio of the flowing fluid is considered constant within
203 the capillary cell with a very short residence time of 0.03s.

204 The performance of scale inhibitor is assessed by injecting scale inhibitor solutions
205 upstream of the mixing point of the waters. The inhibitor was injected into the seawater
206 brine solution containing carbonate ions. The scaling time is first evaluated for the
207 baseline conditions for both the long coil and short capillary cell. The effectiveness of
208 the inhibitor concentration is measured by the time period at which the inhibitor
209 prevents or delays the increase in differential pressure. The concentration of PPCA
210 inhibitor used for the different tests and SI values range from 0.5ppm – 10ppm as in
211 the bottle test for bulk precipitation.

212



213

214

215

216

217

218

Figure 2: (a) Schematic diagram of the capillary rig (b) typical data (Bello, 2017)

219 2.2.3 In-situ visualization cell

220 The in-situ visualization set-up presented in Figure 3, has been described in detail
 221 previously (Sanni et al., 2017). The set-up was designed to work under atmospheric
 222 pressure and allows experimental conditions to be kept constant at the point where
 223 the images are recorded. In addition, the set-up allows surface fouling and bulk
 224 precipitation to be assessed simultaneously. The images captured were processed to
 225 assess the number of crystals and their sizes as well as the CaCO_3 surface coverage.
 226 Similarly, real-time measurements of the bulk precipitation were performed using a
 227 turbidity probe.

228 Prior to the start of the experiment, the thermostatic bath is set to the desired operating
 229 temperature. The two brine solutions are pumped through the thermostatic bath to be
 230 heated up to the desired experimental temperature, they are mixed in a tee chamber
 231 close to the flow cell. The residence time of fluids from the mixing point to the cell is
 232 0.03s at 20ml/min. In the flow cell, the camera takes images of the scale formed on
 233 the substrate every 5 minutes during the course of the experiment.

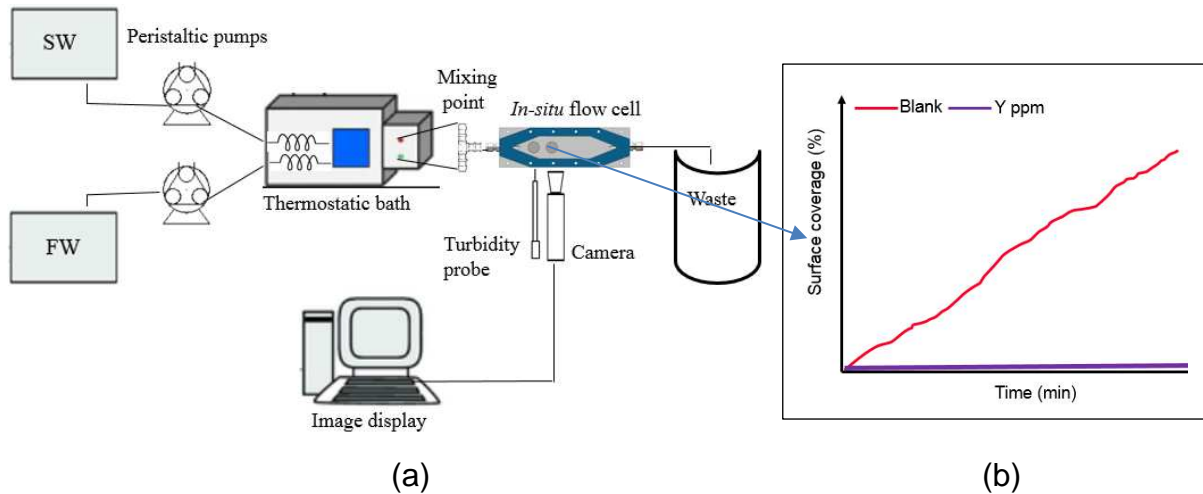


Figure 3: Schematic diagram of the in-situ visualization rig (Sanni et al., 2017)

234
235
236
237

238 The inhibition performances and mechanisms at different SR on both turbidity and
239 surface scaling were assessed in-situ and in real time.

240 CaCO₃ scale inhibition tests were carried out in the flow rig with the two SR values of
241 2.1 and 2.8 at 50°C using polyphosphinocarboxylic acid (PPCA) at 1, 2, 4, 6 and 8ppm.
242 The inhibitor was prepared and added into the seawater (SW) solution, containing
243 CO₃²⁻, prior to mixing.

244 2.3 Test conditions

245 Tests were carried out to assess the effectiveness of each technique regarding scale
246 inhibition. The test conditions for the static and dynamic flow tests are shown in Table
247 3. The temperature used is 50°C to represent a realistic temperature at top side oil
248 production facilities. The flow rate used for the study is 20ml/min and the total time of
249 study is 4hours.

250

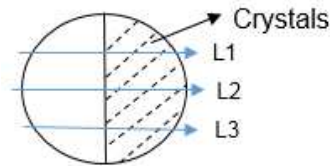
Table 3: Experimental conditions

Parameters	Conditions		
	Bottle	In-situ visualization	Capillary rig
Flow rate (ml/min)	Static	20	
Duration of test (hours)	2 & 22	4	
Mixing Ratio	50:50		
Pressure	Atmospheric		
Temperature (°C)	50		
Inhibitor Concentration (ppm)	1, 2, 4, 6, 8, 10		

251 2.4 Surface profilometry

252 The surface contact profilometer was used to determine the scale thickness or growth
253 in direction normal to the surface (refer to z- direction in the remaining of the paper).
254 The contact profilometer measures the vertical characteristics of the surface deviation.
255 The scale deposition was performed in the visualization rig on four samples under the

256 same condition of saturation index, flow and temperature. The scaling time considered
 257 are 60 minutes, 120 minutes, 180 minutes and 240 minutes corresponding to the
 258 induction period observed in the short capillary (10mm) cell for brine with SI values of
 259 2.1 and 2.8. The scale was deposited on one half of the sample surface while scale
 260 on the other half is prevented with a masking tape. The scale average thickness is
 261 measured relative to the unscaled part of the sample with the evaluation length, L, set
 262 at 8mm at three different sections (Figure 4).

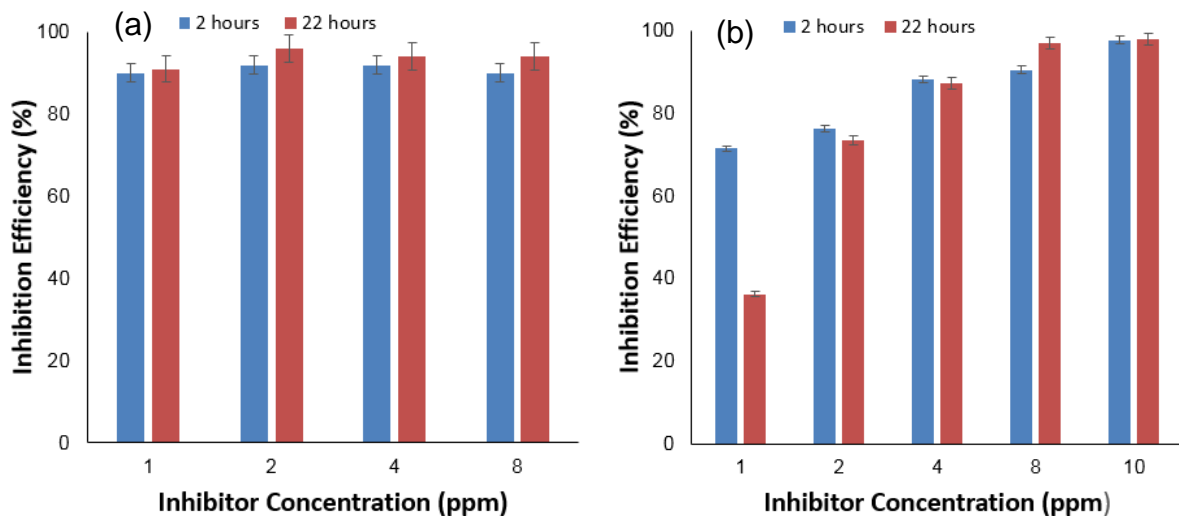


263
 264 Figure 4: Sample profile for surface roughness
 265

266 3 Results and discussion

267 3.1 Bulk Solution Minimum Inhibition Concentration (MIC)

268 The static bottle test was used to establish the bulk MIC for the CaCO₃ brines. The
 269 rate of consumption of ionic species (Ca²⁺, CO₃²⁻) in the bulk solution gives an
 270 understanding of the precipitation rate of calcium carbonate scale (CaCO₃). The MIC
 271 was determined for the brine mixing ratio of NSSW/FW (50:50) at 2 and 22 hours
 272 residence times. The inhibition efficiency at different concentrations of PPCA in the
 273 bulk solutions of CaCO₃ at 50°C are shown in Figure 5. The acceptable industrial
 274 standard for bulk MIC (MIC_{bulk}) is the concentration of inhibitor that gives an 80% or
 275 more inhibition efficiency at 2 and 22 hours (Graham and Sorbie, 1997; Graham et al.,
 276 2001). For this study, the bulk MIC is taken as the concentration level of inhibitor that
 277 maintains a 90% inhibition efficiency. For saturation values of 2.1, the MIC_{bulk} is 1ppm
 278 as the inhibition efficiency is 90%. At SI of 2.8, the 90% efficiency is attained at higher
 279 amount of PPCA concentration of 8 ppm
 280

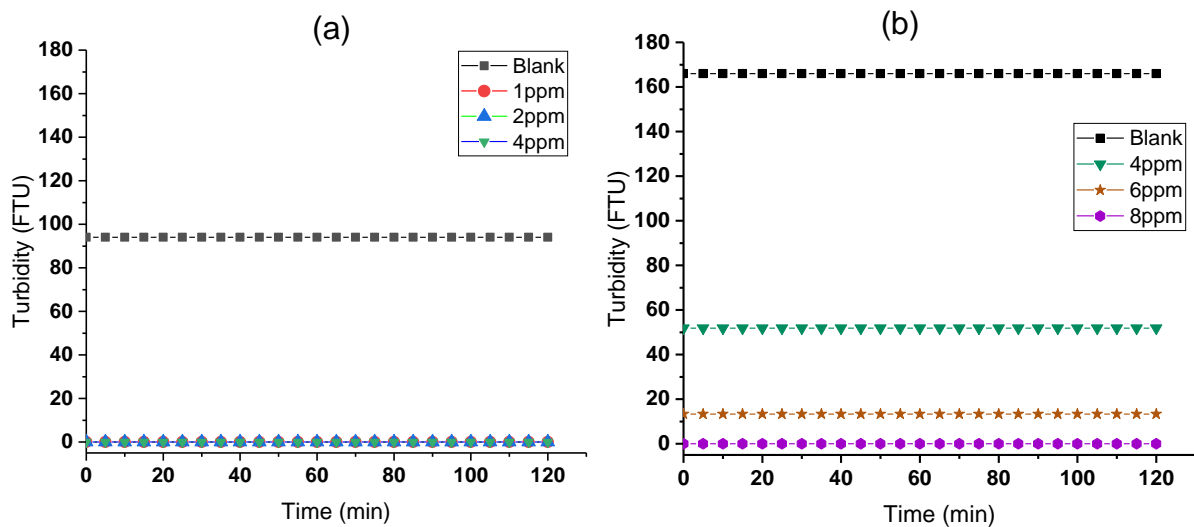


281
 282 Figure 5: Inhibitor efficiency at different levels of scale inhibitor (a) SI = 2.1 (b) SI = 2.8

283 Increase in SI and scaling ions requires greater concentration of PPCA to control the
284 formation of calcium carbonate in the bulk solution. This is consistent with previous
285 results by Graham et al.(Graham et al., 2005; Graham et al., 2001) and (Setta and
286 Neville, 2011)
287

288 3.2 In-situ turbidity measurement

289 The turbidity measurement from the in-situ flow rig for the blank tests plotted in Figure
290 6 are 95 and 166 FTU for SI values of 2.1 and 2.8 respectively with zero induction
291 time. The system is such that the saturation ratio is kept constant throughout the flow
292 cell which consequently maintains constant values of the turbidity measured (Sanni et
293 al., 2017). The inhibition effects and mechanisms for bulk precipitation at different SR
294 were assessed in-situ and in real time. The results presented are in agreement with
295 the MIC_{bulk} obtained from static bottle tests. It can be seen in Figure 6 (a) that for SI
296 value of 2.1, there was no bulk precipitation occurring with the addition of PPCA at
297 1ppm concentration while for SI of 2.8, the bulk scaling is completely inhibited with the
298 injection of 8ppm of PPCA. At these points, the values of the turbidity measured are
299 zero indicating that there are no crystals precipitating in the solution.
300



301
302 Figure 6: In-situ bulk turbidity for (a) SI = 2.1 (b) SI = 2.8
303

304 The real-time in-situ turbidity measurement makes it possible to follow the gradual
305 decrease in turbidity with increasing concentration of PPCA up to the MIC. As shown
306 in Figure 6b, at concentrations below MIC_{bulk} (8ppm), the bulk turbidity values only
307 reduced when compared with the blank turbidity indicating that the precipitation has
308 not been completely controlled.
309

310 3.3 Surface scaling in capillary rig versus conventional tube blocking rig

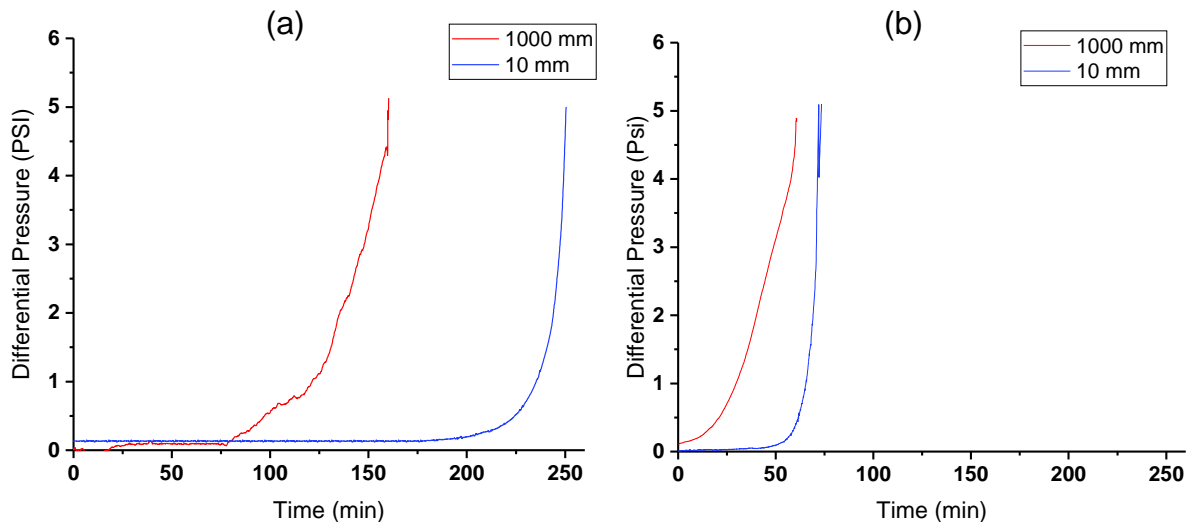
311 The surface scaling times for the uninhibited tests for both the conventional long coil
312 of 1000mm and the adapted short 10mm capillary are presented here. The residence

313 time of the fluid in the long coil is about 3.0s at flow rate of 20 ml/min, and for the short
314 capillary cell, the residence time is 0.025s at the same flow rate of 20 ml/min.

315 For the brine solution with SI value of 2.1 (Figure 7a), the surface scaling induction
316 period is 90 minutes for the conventional tube blocking rig (1000 mm coil length)
317 compared to the induction period of 200 minutes observed for the short capillary rig
318 (10 mm). A similar trend is observed for SI of 2.8, for longer coil length, faster induction
319 time of about 10 minutes and it resulted in faster scale build up as it took shorter time
320 (50 minutes) to reach the threshold differential pressure of 5psi (Figure 7b). However,
321 the induction time for the short capillary for SI 2.8 is observed to be 45 minutes.

322 Homogeneous precipitation and heterogeneous crystallization processes take place
323 in the two cells with a more constant thermodynamic condition in the short capillary.
324 Primary nucleation is a stochastic process which manifests in crystallization at different
325 scales, as such, detection time of crystals may not be identical in many experiments
326 despite identical experimental conditions (Mazzotti, 2015).

327



328

329 Figure 7: Effects of capillary length on scale deposition (a) SI = 2.1, (b) S.I = 2.8
330

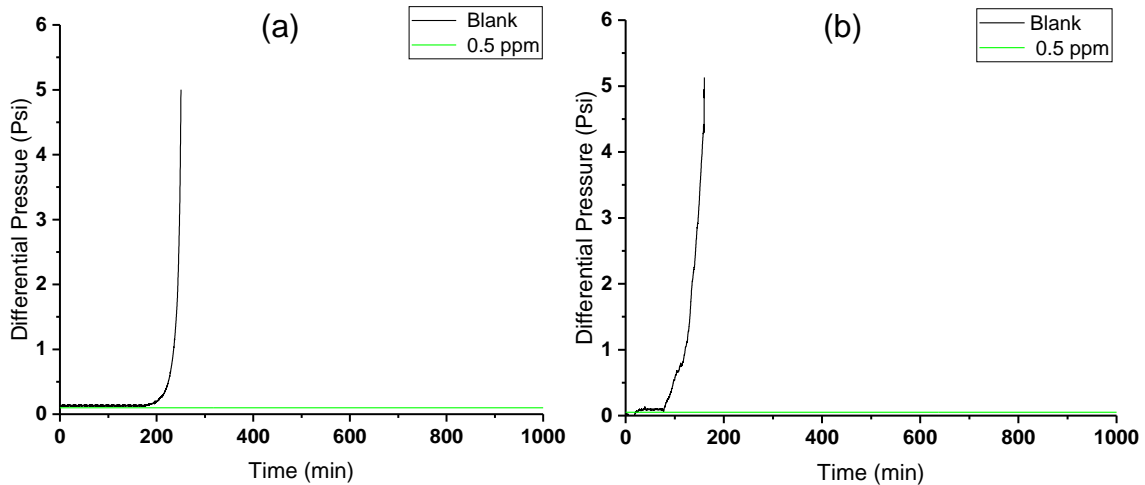
331 The difference in the scaling time observed in these two systems could be attributed
332 to the different lengths and configuration of their cells. The long capillary means
333 greater surface area that can facilitate crystallization by heterogeneous nucleation.
334 Heterogeneous nucleation sites include surface defects, joints and seams in tubing.
335 The hot spots created by the coil system of the long capillary can act as high energy
336 region for surface reaction and could facilitate interaction between the adsorbed
337 hydrated calcium ion and the substrate thereby leading to faster crystallization on the
338 scale (Flaten et al., 2010; Nielsen, 1984; Yamanaka et al., 2012).

339 3.4 Inhibition in capillary rig

340 The capillary rig test is designed to assess scale inhibition under dynamic flow
341 conditions at constant saturation ratio. The Minimum Inhibitor Concentration (MIC) for
342 a given SI is taken as the scaling induction time which corresponds to at least 5 times

343 the blank value (Bazin et al., 2004). The graphs in Figure 8 and Figure 9 summarise
344 the effects of injecting inhibitors to the system.

345 A similar trend is observed with respect to scale inhibition for both the conventional
346 tube blocking and the adapted short capillary systems. For SI 2.1, no scale formation
347 was observed with the addition of 0.5ppm concentration of PPCA while for S.I value
348 of 2.8, the formation of scale in the capillaries was prevented with the injection of 4ppm
349 concentration of PPCA inhibitor.
350

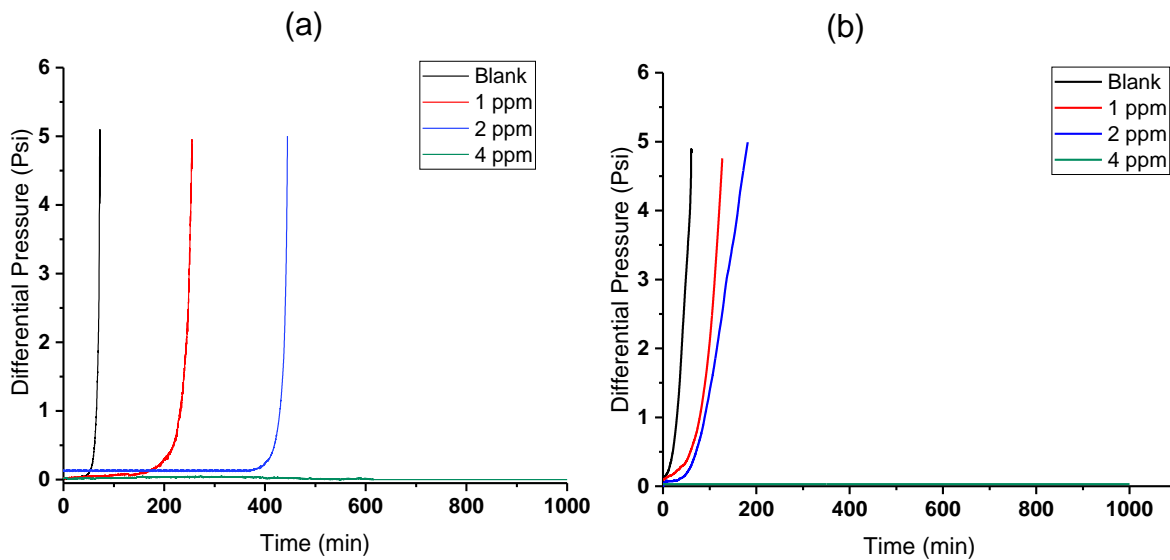


351

352 Figure 8: Scaling in capillary rig at SI = 2.1 (a) Short capillary (b) Long capillary

353

354



355

356 Figure 9: Scaling in capillary rig at SI = 2.8 (a) Short capillary (b) Long capillary

357

358 Results of the inhibition tests from the capillary rig show the concentration of the
359 inhibitor needed to prevent surface scale formation to be lower compared to the static
360 bottle test for bulk. A previous study at 50°C by Graham et al (Graham et al., 2005)
361 reported that the reaction kinetics are moderately fast in the bulk solutions and larger
362 amount of inhibitors were required to control the bulk reaction. The interplay of two or

363 more factors is responsible for the discrepancies between low value of MIC_{surface}
364 obtained from tube blocking test and the high MIC_{bulk} obtained with static bottle test.
365 Firstly, the residence time (0.025s) for the brine solution to travel through the capillary
366 cell after mixing is very short compared to the long residence times (2 hours, 22 hours)
367 used for the standard bottle test (Graham and Sorbie, 1997). The longer residence
368 time of bottle test would promotes growth of crystals at later stages. It is erroneous to
369 make a direct comparison of MIC between the two systems as the parameters may
370 vary and the residence times differ. Secondly, the chemistry of inhibitors which make
371 them efficient in stopping either nucleation or growth of crystals with PPCA regarded
372 as being more effective nucleation inhibitors (Reddy and Hoch, 2001; Yuan et al.,
373 1998). The short residence time of brine solution in the capillary cell and long coil
374 coupled with the effective nucleation inhibiting mechanisms of PPCA, the nucleation
375 sites are reduced significantly, the differential pressure would be held at zero or rise
376 slowly depending on the SI and concentrations of inhibitors.

377
378 Employing the MIC determined from the tube blocking rig may pose a potential
379 problem both with regards to scaling in bulk and surface facilities as surface growth of
380 nucleated crystals can still take place at a slow rate. Previous studies have shown
381 surface MIC (MIC_{surface}) to be higher than MIC_{bulk} (Bukuaghangin et al., 2015; Chen et
382 al., 2004; Graham and Sorbie, 1997; Graham et al., 2005; Setta and Neville, 2011).
383 Surface deposition is usually initiated by heterogeneous nucleation which requires a
384 lower energy barrier than the homogenous nucleation in bulk precipitation (Myerson,
385 2001; Setta and Neville, 2011). The growth of scale on metal surfaces is clearly a
386 much more serious problem than precipitation within the bulk solution.

387 3.5 Surface scaling and inhibition using in-situ visualization

388 The in-situ flow visualization set up has been used to assess surface deposition and
389 inhibition under the same set of conditions in the capillary rig. The range of inhibitor
390 concentration, SI values, flow rates and temperature are maintained as in the capillary
391 rig test.

392 3.5.1 In-situ surface images

393 The in-situ images for each set of experimental condition were recorded every 5
394 minutes for 4 hours. Figure 10 shows surface crystals formed after 10 minutes and
395 240 minutes at SI value of 2.1 without inhibitor. The constant SI means that the
396 thermodynamic condition is constant across the cell, as such, surface growth and bulk
397 precipitation can be observed to continue over the duration of the experiment with
398 larger crystals and more surface coverage at 240 minutes.

399
400

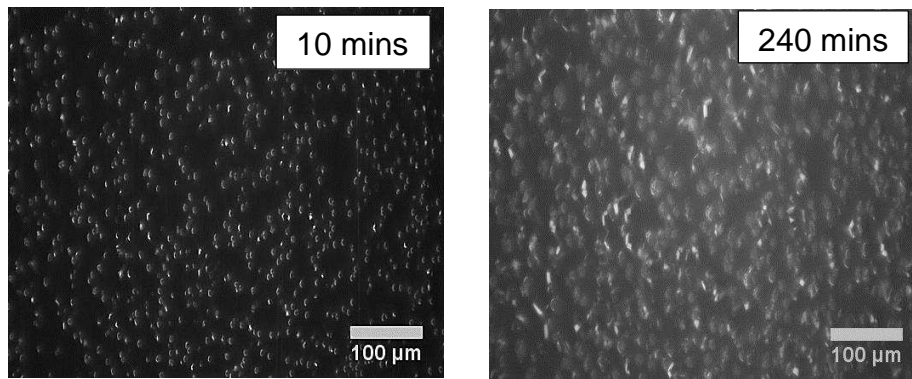


Figure 10: In-situ surface images for Blank test at SR = 2.1

401
402
403

404 The number of crystals formed on the surface is reduced with the injection of 1ppm
405 inhibitor. This is the MIC_{bulk} determined from the bottle test and also effective to control
406 the in-situ bulk precipitation in the visualization rig. However, contrary to assessment
407 of surface inhibition using the capillary rig, it is shown with the in-situ surface images
408 in Figure 11 that the active surface nucleation sites are only reduced but the growth of
409 already nucleated crystals continued. Real time visualization test in contrast to the
410 capillary tests shows that complete inhibition of surface scaling was not achieved at
411 1ppm concentration. At this concentration, the inhibitor molecules are not completely
412 adsorbed and block all the active growth sites to prevent growth of the crystals
413 (Bukuaghangin et al., 2016; Graham and Sorbie, 1997; Graham et al., 2004) .

414

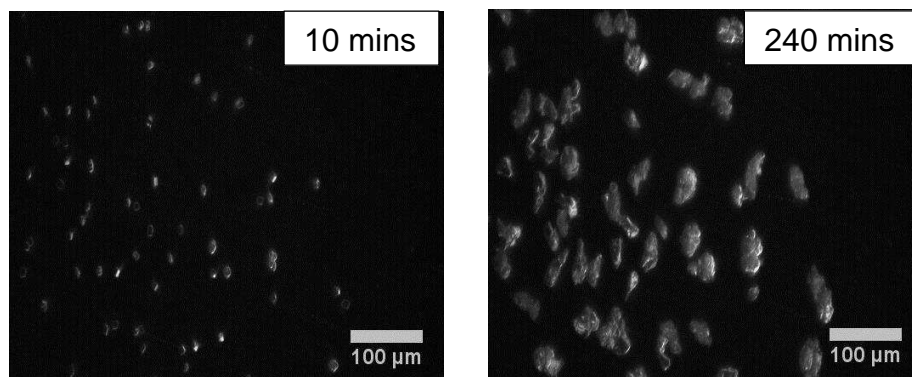
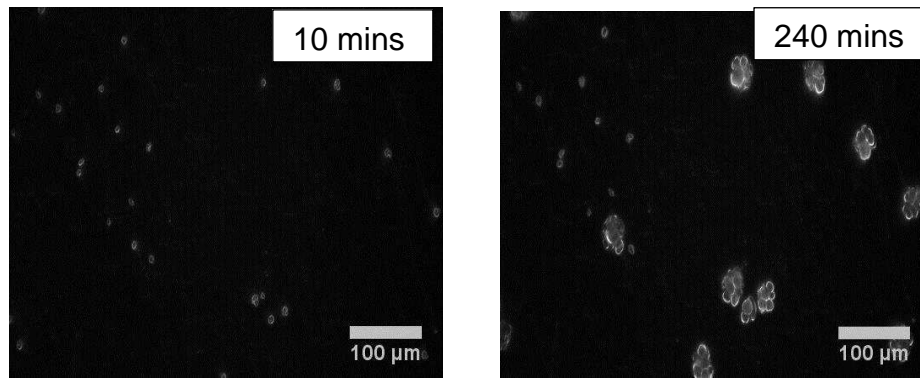


Figure 11: In-situ surface images at SR = 2.1 and 1ppm PPCA

415
416

417 Further increase in the concentration of PPCA to 2ppm resulted in greater reduction
418 in the number of crystals as shown in Figure 12. Here, more crystals growth's sites
419 are blocked compared to 1ppm concentration of PPCA concentration. The scale
420 formation at the surface is significantly diminished but not entirely controlled at
421 concentration slightly above the MIC_{bulk} . The overall surface coverage was significantly
422 reduced and could be accountable for the inability of the capillary rig to detect the
423 surface scaling at the same concentration of PPCA.

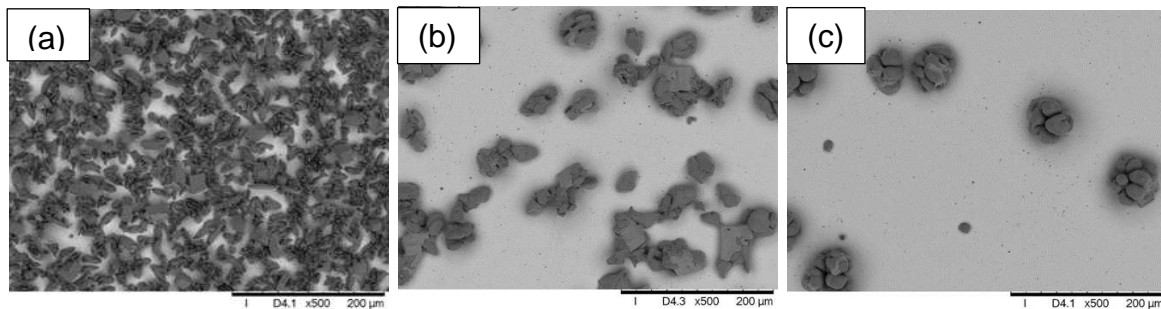
424



425
426
427
428
429
430
431
432
433
434
435
436
437

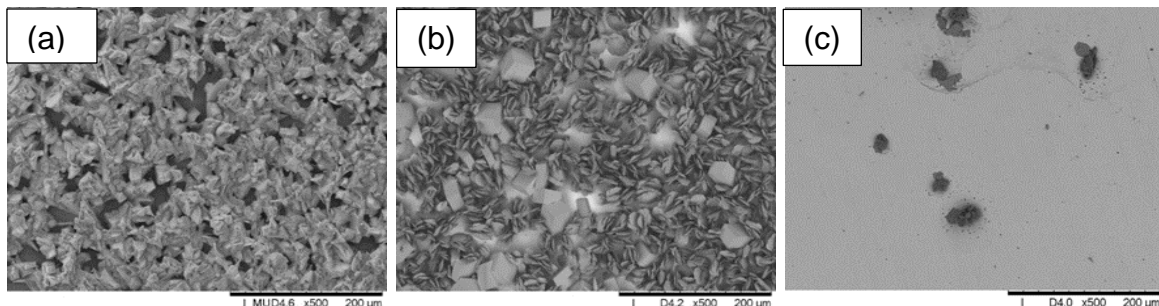
Figure 12: In-situ surface images at SR = 2.1 and 2ppm PPCA

Scanning Electron Microscope (SEM) images were taken to assess the morphology of the surface crystals formed on the samples in the in-situ cell after 4 hours. Figure 13 and Figure 14 show the SEM images for SI = 2.1 and 2.8 respectively at flow rate of 20 ml/min. For the uninhibited test, the crystals are distributed uniformly across the metal surfaces. The crystals are composed of mainly leaf-like vaterite and a few sparsely distributed cubic calcite crystals which is consistent with previous works on CaCO₃ deposition at 50°C (Euvrard et al., 2000; Kjellin, 2003; Sanni et al., 2017). However, injection of inhibitors at MIC_{bulk} resulted in distorted growth of the surface crystals because the inhibitor molecules are not completely adsorbed on all faces resulting in preferential growth of faces (Bukuaghangin et al., 2016; Mavredaki, 2009).



438
439
440
441

Figure 13: SEM images of the CaCO₃ scale deposited on the surface for SI = 2.1 at 50°C; (a) blank (b) 1ppm PPCA (c) 2ppm PPCA



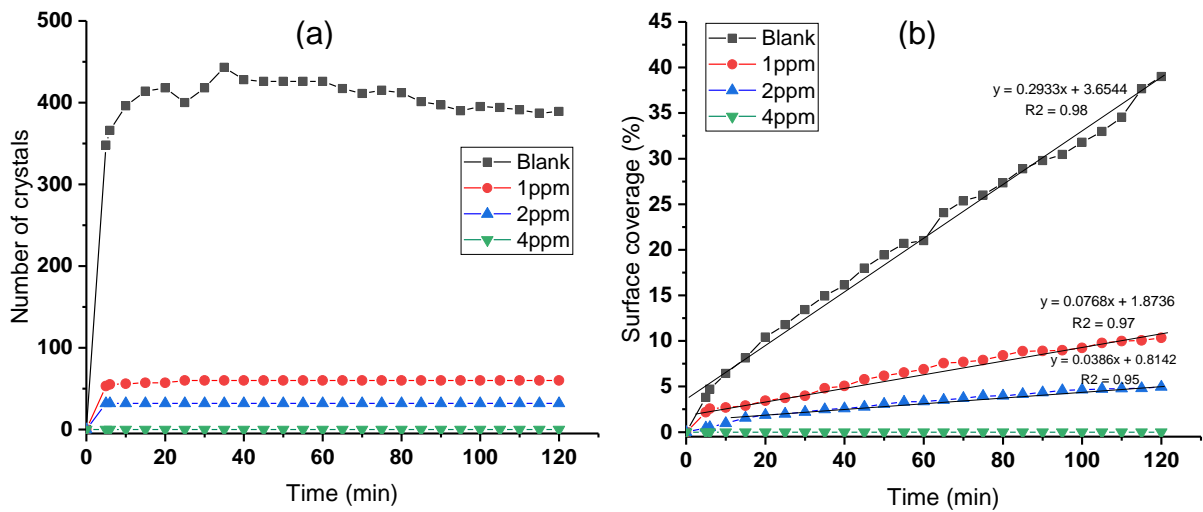
442
443
444
445

Figure 14: SEM images of the CaCO₃ scale deposited on the surface for SI = 2.8 at 50°C; (a) blank (b) 4ppm PPCA (c) 8ppm PPCA

446 3.5.2 Crystal nucleation and surface coverage

447 The in-situ images from the visualization rig were analysed to assess the number and
448 the surface coverage of crystals. In all cases, the crystals could be quantified as soon
449 as their sizes reached 1µm. Figure 15 presents the reduction in surface nucleation
450 and total surface coverage of scale as PPCA concentration is increased from 1ppm,
451 2ppm to 4ppm for SI of 2.1.

452 Generally, the number of crystals decreases with increase in the concentration of
453 PPCA inhibitor. The PPCA acts to block active nucleation sites and consequently
454 inhibits scale formation to various degrees depending on its concentration and brine
455 solution SI.

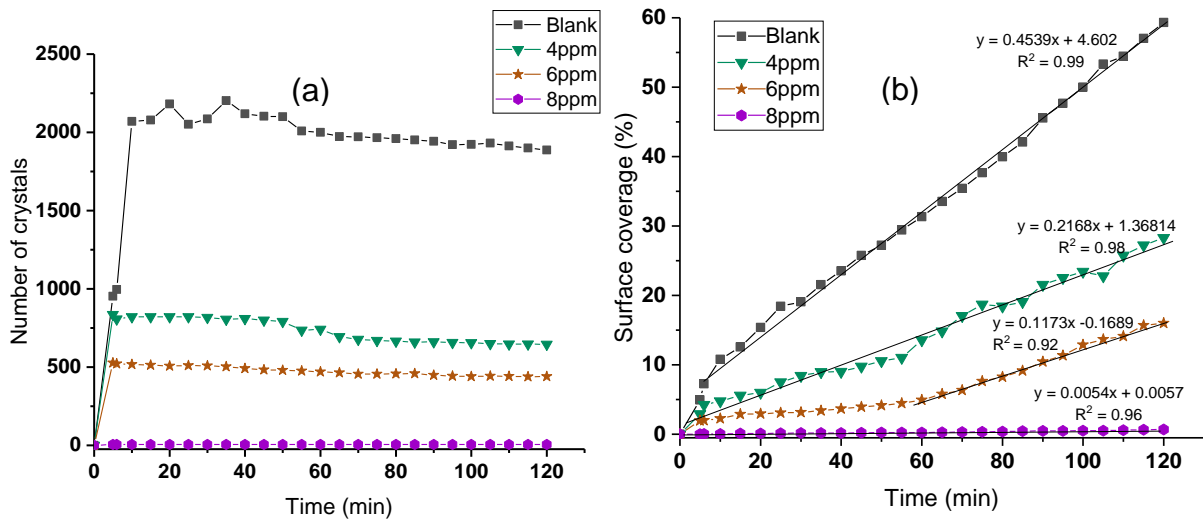


456

457 Figure 15: (a) Number of crystals and (b) Surface coverage at SR = 2.1 for blank and with PPCA
458 inhibitor at different concentrations
459

460 For SI value of 2.1 (Figure 15), the inhibitor concentration required to effectively inhibit
461 scaling is 4ppm compared to the capillary rig test where the concentration is 1ppm for
462 the same SI. The visualization rig technique shows that nucleation of crystals is only
463 partially inhibited with the injection of 1ppm and 2ppm of PPCA inhibitor, and the rates
464 of surface coverage are only significantly reduced with respect to the non-inhibited test
465 as shown in Figure 15b. Nucleation of crystals is completely inhibited when 4ppm of
466 PPCA was added as no crystals are detected, therefore the surface coverage remains
467 at zero. At this concentration, heterogeneous surface nucleation was totally controlled
468 with complete adsorption of inhibitor molecules on the nucleation sites.

469



470

471 Figure 16: (a) Number of crystals and (b) Surface coverage at SR = 2.8 for blank and with PPCA
 472 inhibitor at different concentrations
 473

474 For higher SI of 2.8 (Figure 16a), the inhibitor concentration of 4ppm was not sufficient
 475 to block all the nucleation sites. The number of active nucleation sites is a function of
 476 SI, therefore, a function of the ionic concentration of the brine solutions. Here, higher
 477 PPCA inhibitor concentration of 8ppm is required to completely inhibit crystal growth.
 478 This is in contrast to the capillary rig test where no increase in differential pressure
 479 was observed with the addition of PPCA at 4ppm. The results from the visualization
 480 rig in Figure 16 shows that at this concentration (4ppm), the number of crystals was
 481 only reduced while the rate of surface coverage of scale significantly dropped from
 482 $0.29 \mu\text{m}^2/\text{min}$ to $0.04 \mu\text{m}^2/\text{min}$. PPCA partially inhibits calcium carbonate nucleation
 483 by decreasing the number of nuclei and also the number of active sites on the metal
 484 (Martinod, 2008).

485 Thus, MIC levels depend on the sensitivity that can be achieved in the different rigs.
 486 The visualization set up could be used to evaluate the minimum inhibitor concentration
 487 at which complete inhibition of scaling on surface equipment is achievable. This is
 488 usually higher than the MIC require to delay the surface induction or scaling time as
 489 determined by the dynamic tube blocking rig. The concentration requires to completely
 490 inhibit further growth is a function of percentage surface coverage of crystals and the
 491 number of active growth sites. With greater surface coverage, it requires higher
 492 concentration of the inhibitor to be completely adsorbed on the crystals.

493 The effects of injecting the PPCA inhibitor on the kinetics is summarised in Table 4.
 494 The rate of scale formation is the slope of the linear fit on the surface coverage area
 495 (Figure 15 and Figure 16) as a function of time.

496

497

Table 4: Rate of surface coverage with inhibitor injection at S.I = 2.1 and 2.8

SR	Inhibitor Concentration	Linear Equation	Rate ($\mu\text{m}^2/\text{s}$)
2.1	Blank	$y = 0.293x + 3.654$	0.293
	1 ppm	$y = 0.077x + 1.874$	0.077
	2 ppm	$y = 0.038x + 0.814$	0.038
	4 ppm	$y = 0.000$	0.000
2.8	Blank	$y = 0.454x + 4.602$	0.454
	1 ppm	$y = 0.216x + 1.368$	0.216
	2 ppm	$y = 0.112x - 0.1698$	0.112
	4 ppm	$y = 0.005x + 0.005$	0.005

499

500 Higher SR shows higher rates of surface scale coverage while a decrease in rate of
 501 formation is clearly observed with an increase in the concentration of inhibitors. This
 502 shows that the adsorption rate of inhibitors is a function of its concentration. The in-
 503 situ technique allows to know the concentration that completely inhibit surface scaling,
 504 in this case, 4ppm was able to block all the active sites at S.I value of 2.1 and prevent
 505 nucleation of crystals.

506 In regards to the crystallization mechanisms, it can be observed from Figures 15a and
 507 16a that nucleation takes place very fast with no measurable induction period
 508 (Karabelas, 2002) and the number of crystals stabilizes very quickly. The nucleation
 509 mechanisms is instantaneous nucleation as all active nucleation sites are assumed to
 510 be converted into nuclei at the early stage of crystallization (Beaunier et al., 2001;
 511 Euvrard et al., 2006). The nucleation process did not proceed for the entire duration
 512 of the test. The number of crystals reaches a maximum, as such, the later stages of
 513 crystallization process would be dominated by the growth or agglomeration of existing
 514 crystals as indicated by the increase in surface coverage with time (Figure 15b and
 515 Figure 16b). It shows that a scaling surface consists of a finite number of active
 516 nucleation sites (Beaunier et al., 2001).

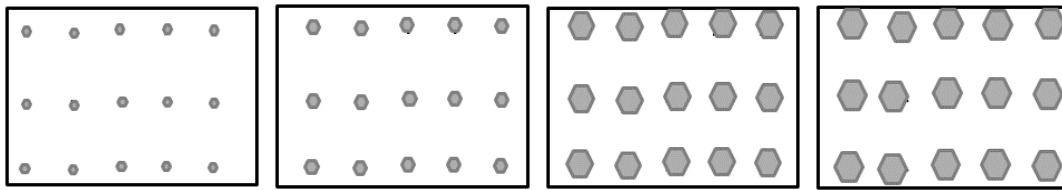
517 As stated in equation (1), for instantaneous nucleation:

$$S(t) = \frac{MK_1 N_o t}{\rho}$$

518 Therefore, plotting the actual surface coverage, $S(t)$ against time, t for SI values of 2.1
 519 and 2.8 gives a linear relationship as shown in Figure 15b and Figure 16b.

520 The CaCO_3 crystals are formed in a short time and grow progressively as a result of
 521 constant supersaturation as shown in Figure 17. The early stage of crystallization is
 522 dominated by rapid nucleation with all available active sites generating nuclei in a
 523 relatively short period (Sanni et al., 2016). This is similar to the observations by

524 Beaunier et al (Beaunier et al., 2001) for high concentrations of calcium ions where it
 525 was assumed that diffusion controls the process.



526
 527 Figure 17: Schematic illustration of instantaneous crystallization mechanisms

528 There are different mechanisms to control the process of scale formation at different
 529 ionic concentrations. The ability to understand and determine the surface
 530 crystallization mechanisms allows for the correct type and dosage of inhibitor to be
 531 selected. It could also help to assess how efficient inhibitors would be in controlling
 532 either the nucleation or growth of scale on surfaces. Inhibition strategy should be able
 533 to accommodate the possibility of surface scaling without bulk precipitation and the
 534 use of either nucleation or growth inhibitors.

535

536 3.6 Minimum Inhibition Concentration from the different test methods

537 The minimum inhibitor concentrations obtained for each technique is summarised in
 538 Table 5.

539

540 Table 5: Minimum inhibition concentration (MIC) values from different techniques

Technique	Bulk Precipitation		Surface crystallization	
	SI 2.1	SI 2.8	SI 2.1	SI 2.8
Bottle jar test	1	8	-	-
TBT Long	-	-	0.5	4
TBT Short	-	-	0.5	4
Visualization test (VR)	1	8	4	>8

541

542 The MIC_{bulk} determined from bottle test and supported with the in-situ turbidity MIC_{bulk}
 543 for SI of 2.1 and SI of 2.8 are 1ppm and 8ppm respectively. It requires a considerably
 544 lower concentration of PPCA for the surface inhibition test using the capillary rig. The
 545 method for assessing the efficiency of scale inhibitor varies in the two systems. Scale
 546 inhibition efficiency is measured in terms of the reduction of scaling ion concentrations
 547 for static bottle test while it is expressed in terms of delaying the induction time up to
 548 5 times of the blank scaling time in the capillary rigs. By comparison, the longer
 549 residence time in static bottle test could result in further growth of nucleated crystals
 550 which invariably require higher concentration of inhibitor for maximum efficiency than
 551 the capillary rig (Graham and Sorbie, 1997). The consumption of inhibitor by
 552 adsorption within the lattice of growing crystals leads to a reduction in its concentration

553 and consequently restricts its ability to prevent further growth. The dynamic condition
554 in the tube blocking rig can also magnify a possible dispersion mechanisms in addition
555 to nucleation inhibiting mechanisms, since the scale inhibition and differential pressure
556 rise is determined by the build-up of scales on the wall of the tubing (Graham and
557 Sorbie, 1997).

558 The surface visualization methods enables the range of concentration of inhibitors at
559 which both bulk and surface scaling are completely controlled to be determined. MIC
560 in the visualization cell is defined as the concentration of inhibitors which prevent
561 surface crystallization completely by blocking all the active nucleation sites. The
562 surface inhibition from the in-situ visualization rig shows the surface MIC at SI values
563 of 2.1 and 2.8 is 4ppm and 8ppm respectively. The visualization rig as compared with
564 the capillary rig shows that surface inhibition requires higher concentrations to reach
565 PPCA inhibition efficiency. In agreement with previous study, the calcium carbonate
566 inhibition requires higher concentrations for surface scaling than for bulk scale
567 precipitation. The formation of surface scale is as a result of heterogeneous process
568 compared to scale precipitation which originally starts as a homogeneous reaction in
569 a bulk free of suspended particles (Setta and Neville, 2011). The inhibitor
570 concentrations needed to suppress CaCO_3 scale precipitation are generally not
571 enough to prevent CaCO_3 deposition on a stainless steel surface due to the different
572 mechanisms and kinetics involved in these two processes (Cheong et al., 2012;
573 Morizot and Neville, 2001; Sanni et al., 2017).

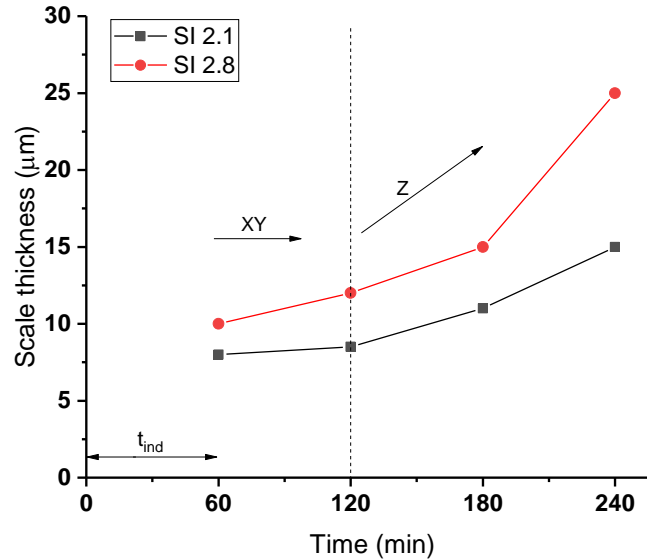
574 MIC cannot be viewed in isolation. It depends on whether scale formation is to be
575 completely prevented as in the case of downstream safety control valves or
576 controlled/reduced as in pipelines. It is important to ascertain whether the application
577 of inhibitor is actually meant to achieve a delay of induction period or to effectively stop
578 the growth of crystals. For this, there needs to be an understanding of the tolerable
579 level of scale and often this is very difficult to determine.

580 The $\text{MIC}_{\text{surface}}$ from capillary test which effectively delayed the induction time
581 throughout the experiment is considerably lower than the $\text{MIC}_{\text{surface}}$ from the
582 visualization test. At the $\text{MIC}_{\text{surface}}$ from the capillary test, the visualization cell shows
583 that surface growth continues, albeit at a lower rate. The difference in $\text{MIC}_{\text{surface}}$
584 between the capillary rig and the in-situ visualization rig can be due to the sensitivity
585 and capabilities of the two techniques. It emphasises the need to understand each
586 technique and their limitations in order to predict scale formation and evaluate its
587 control using inhibitor.

588 3.7 In-situ visualization versus capillary tests - Thickness of scale deposits

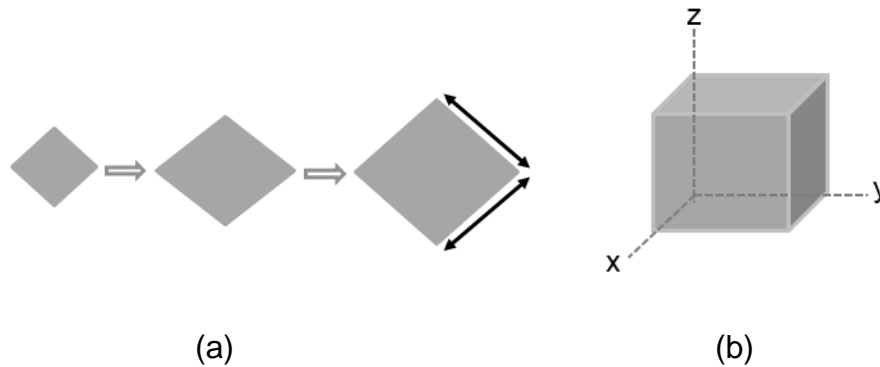
589 The surface scale deposition were further analysed by profilometry technique to
590 assess the thickness of scale formed with time on the surface. Estimating the scaling
591 kinetics would be difficult using the Hagen-Poiseuille flow equation (Jianxin wang,
592 2004; Kazeem A. Lawal, 2012; Zhang et al., 2001) especially for the longer coil where
593 there is a drop in the saturation ratio across the capillary cell due to longer residence

594 time. The scale layer is not uniform, and as such to link the deposition thickness to the
 595 pressure drop along the capillary tube based on Hagen-Poiseuille equation will not be
 596 valid. Figure 18 shows the surface thickness, which is a measure of the vertical
 597 characteristics of the surface deviation as a function of time. It distinguished the stages
 598 of growth clearly detected by both the in-situ visualization and capillary cells.



599
 600 Figure 18: Surface thickness of deposits
 601

602 The induction period is followed by an early stage of crystallization up to about 120
 603 minutes where the growth is parallel to the surface and increasing the scale coverage.
 604 The growth of the crystals at the initial stage is basically on the XY plane as depicted
 605 in Figure 19a.



606
 607
 608 (a) (b)
 609 Figure 19: Schematic representation of the growth of scale during (a) Initial (b) later stages of
 610 crystallization process.
 611

612 This is the region where the in-situ visualization is more practically suitable to detect
 613 and analyse crystallization processes comprising of induction, nucleation and the early
 614 stages of growth. For the capillary rig, this initial stage corresponds to the surface
 615 induction period (Figure 7) where the differential pressure remains at zero. However,
 616 the surface induction time from the capillary test is different when compared to the in-
 617 situ visualization test. The surface induction time for the visualization test is taken as
 618 the time for the first crystal to be detected on the surface. Scale crystals are already

619 detected with the in-situ visualization cell for the period of induction indicated in the
620 capillary test. The critical nuclei are not detected when formed upon nucleation in the
621 capillary test until after growing to a size large enough to occupy a significant volume
622 fraction of the cell.

623

624 At the later stages of crystallization, the scale start to grow in the z-direction which
625 increases the scale thickness as depicted in Figure 18b. This second stage is observed
626 to coincide with the time or point where there is a rise in differential pressure in the
627 capillary test (Figure 7). At the later stage of growth, the scale deposition could not be
628 easily analysed with the visualization rig as the crystals begin to cluster and grow out
629 of focus. The visualization rig would therefore be best for detecting and assessing
630 early stages of surface crystallization. The analysis shows that the scaling or induction
631 time for the dynamic tube blocking rig could actually be the onset of growth in the z-
632 direction.

633 A good understanding of the mechanisms of bulk and surface scaling processes can
634 enable reliable strategies for mitigating its formation in the field to be developed. A
635 knowledge of the mechanisms is required to predict scale formation and its control
636 using inhibitor, therefore, scale inhibitor selection and ranking for a proposed field
637 application can be made more effective by employing laboratory test techniques that
638 will better simulate and reflect the real field scaling environment that the inhibitor will
639 encounter on application.

640

641 **4 Conclusions**

642 The work has shown the uniqueness and suitability of the various techniques including
643 a recently developed in-situ visualization rig to distinctively quantify the inhibition of
644 both nucleation and growth of surface scaling. The use of shorter capillary length
645 instead of the more conventional long coil of the tube blocking system allows to keep
646 the experimental conditions constant across the working section.

647 The determination of the correct dosage or minimum inhibition concentration (MIC) to
648 effectively combat scale problems relies amongst other factors, on the accuracy,
649 sensitivity or effectiveness of the techniques employed. It points to a potential
650 problems if viewed in isolation. Each technique has its merits and contributes specific
651 performance data that could provide the basis for scale mitigation when viewed
652 together. There is no single test design which can successfully stimulate all possible
653 field scenarios. Bottle test, capillary test (dynamic tube blocking test) and the new in-
654 situ visualization method offer complementary information to study crystallization and
655 inhibition of sparingly soluble salts.

656

- 657 • The standard bottle test provides useful data regarding the threshold below
658 which scale precipitation is likely to occur. It also emphasises the efficiencies
659 of chemical inhibitors to prevent homogeneous bulk crystallization.

- 660 • The capillary and dynamic tube blocking tests provide more insight on the
661 kinetics of crystal growth in Z direction, relating to the later stages of
662 crystallization.
- 663 • The in-situ visualization cell is effective to study early stage surface
664 crystallization, when the growth is in the XY plane. The scale is typically single
665 layer of crystals and can offer a good evaluation of nucleation inhibitors. It also
666 offers a close assessment of both bulk and surface scaling inhibition
667

668 A good understanding of the mechanisms of bulk and surface scaling processes could
669 enable reliable strategies for mitigating its formation in the field to be developed.
670 Information needed to ascertain the performance of scale inhibitors should not be
671 based only on their performance under various environmental conditions such as
672 temperature, pH, hydrodynamic conditions and brine composition but also where
673 possible on data from two or more techniques.
674

675 **Acknowledgement**

676 The authors acknowledge the funding and support from the Flow Assurance and Scale
677 Team (FAST) consortium and the Leverhulme Trust Research Grant ECF-2016-204.
678 We also wish to appreciate the technical and administrative team of the Institute of
679 Functional Surfaces (IFS), School of Mechanical Engineering at the University of
680 Leeds for their supports.

681

682 **Reference**

- 683 Amjad, 1998. Water Soluble Polymers Solution Properties and Applications. Springer-
684 Verlag.
- 685 Amjad, Z., 1994. Inhibition of barium sulfate precipitation: Effects of additives, solution
686 pH, and supersaturation. *Water Treatment*, 9(1): 47-56.
- 687 Bazin, B., Kohler, N. and Zaitoun, A., 2005. Some Insights Into the Tube-Blocking-
688 Test Method To Evaluate the Efficiency of Mineral Scale Inhibitors, SPE Annual
689 Technical Conference and Exhibition. Society of Petroleum Engineers, Dallas,
690 Texas.
- 691 Bazin, B., Kohler, N., Zaitoun, A., Johnson, T. and Raaijmakers, H., 2004. A New Class
692 of Green Mineral Scale Inhibitors for Squeeze Treatments, SPE International
693 Symposium on Oilfield Scale. Society of Petroleum Engineers, Aberdeen,
694 United Kingdom, pp. 12.
- 695 Beaunier, L., Gabrielli, C., Poindessous, G., Maurin, G. and Rosset, R., 2001.
696 Investigation of electrochemical calcareous scaling: Nuclei counting and
697 morphology. *Journal of Electroanalytical Chemistry*, 501(1-2): 41-53.
- 698 Bello, O., 2017. Calcium Carbonate Scale Deposition Kinetics on Stainless Steel
699 Surface. University of Leeds PhD Thesis.
- 700 Boak, L.S., Graham, G.M. and Sorbie, K.S., 1999. The Influence of Divalent Cations
701 on the Performance of BaSO Scale Inhibitor Species, SPE International

- 702 Symposium on Oilfield Chemistry. Society of Petroleum Engineers, Houston,
703 Texas.
- 704 Bukuaghangin, O., Neville, A. and Charpentier, T., 2015. Scale Formation in
705 Multiphase Conditions, Proceedings of the Oil Field Chemistry Symposium,
706 Gielo.
- 707 Bukuaghangin, O. et al., 2016. Kinetics study of barium sulphate surface scaling and
708 inhibition with a once-through flow system. Journal of Petroleum Science and
709 Engineering, 147: 699-706.
- 710 Charpentier, T.V.J. et al., 2015. Liquid infused porous surfaces for mineral fouling
711 mitigation. Journal of Colloid and Interface Science, 444: 81-86.
- 712 Chen, T., Neville, A. and Yuan, M., 2004. Assessing the effect of Mg^{2+} on $CaCO_3$ scale
713 formation - bulk precipitation and surface deposition. crystal growth, 275: 1341-
714 1347.
- 715 Chen, T., Neville, A. and Yuan, M., 2005. Calcium carbonate scale formation -
716 Assessing the initial stages of precipitation and deposition. Journal of
717 Petroleum Science and Engineering, 46(3): 185-194.
- 718 Chen, T.N., Anne; Yuan, Mingdong; Sorbie, Ken, 2005. Influence of PPCA inhibitor on
719 $CaCO_3$ scale surface deposition and bulk precipitation at elevated temperature
720 Research gateway, 15(09): 35-41.
- 721 Cheong, W.C., Gaskell, P.H. and Neville, A., 2012. Substrate effect on surface
722 adhesion/crystallisation of calcium carbonate. Journal of Crystal Growth, 363:
723 7-21.
- 724 Dyer, S. and Graham, G.M., 2002. The Effect of Temperature and Pressure on Oilfield
725 Scale formation. Petroleum Science and Technology, 35: 95-97.
- 726 Euvrard, M., Filiatre, C. and Crausaz, E., 2000. Cell to study in situ
727 electrocrystallization of calcium carbonate. Journal of Crystal Growth, 216(1):
728 466-474.
- 729 Euvrard, M., Membrey, F., Filiatre, C., Pignolet, C. and Foissy, A., 2006. Kinetic study
730 of the electrocrystallization of calcium carbonate on metallic substrates. Journal
731 of Crystal Growth, 291(2): 428-435.
- 732 Farooqui, N.M., Grice, A., Sorbie, K.S. and Haddleton, D., 2014. Polyphosphino
733 Carboxylic Acid (PPCA) Scale Inhibitor for Application in Precipitation Squeeze
734 Treatments: The Effect of Molecular Weight Distribution, CORROSION 2014.
735 NACE International, San Antonio, Texas, USA, pp. 16.
- 736 Flaten, E.M., Seiersten, M. and Andreassen, J.-P., 2010. Growth of the calcium
737 carbonate polymorph vaterite in mixtures of water and ethylene glycol at
738 conditions of gas processing. Journal of Crystal Growth, 312(7): 953-960.
- 739 Frenier, W., M. Ziauddin, 2008. Formation, removal, and inhibition of inorganic scale
740 in the oilfield environment. Society of Petroleum Engineers
741 Journal(1555631401): 1-230.
- 742 Graham and Sorbie, a.J., 1997. How Scale Inhibitors Work and How this Affects Test
743 Methodology. Presented at the 3rd International Conference on Advances in
744 Solving Oilfield Scaling, Aberdeen.

- 745 Graham, A.L., Boak, L.S., Neville, A. and Sorbie, K.S., 2005. How Minimum Inhibitor
746 Concentration (MIC) and Sub-MIC Concentrations Affect Bulk Precipitation and
747 Surface Scaling Rates, SPE International Symposium on Oilfield Chemistry.
748 Society of Petroleum Engineers, The Woodlands, Texas.
- 749 Graham, A.L., Vieille, E., Neville, A., Boak, L.S. and Sorbie, K.S., 2004. Inhibition of
750 BaSO₄ at a Hastelloy Metal Surface and in Solution: The Consequences of
751 Falling Below the Minimum Inhibitor Concentration (MIC), SPE International
752 Symposium on Oilfield Scale. Society of Petroleum Engineers, Aberdeen,
753 United Kingdom.
- 754 Graham, G.M., Boak, L.S. and Hobden, C.M., 2001. Examination of the Effect of
755 Generically Different Scale Inhibitor Species (PPCA and DETPMP) on the
756 Adherence and Growth of Barium Sulphate Scale on Metal Surfaces,
757 International Symposium on Oilfield Scale. Society of Petroleum Engineers,
758 Aberdeen, United Kingdom.
- 759 Jianxin wang, J.S.B., and Jefferson L. Creek, , 2004. Asphaltene Deposition on
760 Metallic Surfaces. *Journal of Dispersion Science and Technology*, 25: 287 -
761 298.
- 762 Karabelas, A.J., 2002. Scale formation in tubular heat exchangers—research
763 priorities. *International Journal of Thermal Sciences*, 41(7): 682-692.
- 764 Kazeem A. Lawal, J.P.C., Edo S.Boek, and Velisa Vesovic, , 2012. Experiemntal
765 Investigation of Asphaltene Deposition in Capillary Flow. *energy & fuels*.
- 766 Keogh, W. et al., 2017. Deposition of Inorganic Carbonate, Sulfate and Sulfide Scales
767 on Anti-fouling Surfaces in Multiphase Flow, 31.
- 768 Kjellin, P., 2003. X-ray diffraction and scanning electron microscopy studies of calcium
769 carbonate electrodeposited on a steel surface. *Colloids and Surfaces A:
770 Physicochemical and Engineering Aspects*, 212(1): 19-26.
- 771 Koutsoukos, P.G. and Kontoyannis, C.G., 1984. Prevention and inhibition of calcium
772 carbonate scale. *Crystal Growth*, 69(2-3): 367-376.
- 773 Liu, X. et al., 2012. Understanding Mechanisms of Scale inhibition Using Newly
774 Developed Test Method and Developing Synergistic Combined Scale
775 Inhibitors, SPE International Conference on Oilfield Scale. Society of Petroleum
776 Engineers, Aberdeen, UK.
- 777 Liu, Y. et al., 2016. An assay method to determine mineral scale inhibitor efficiency in
778 produced water. *Journal of Petroleum Science and Engineering*, 143: 103-112.
- 779 Martinod, A., et al., 2008. Progressing the understanding of chemical inhibition of
780 mineral scale by green inhibitors. *Desalination*, 220: 345-352.
- 781 Mavredaki, E., 2009. Barium Sulphate Formation Kinetics and Inhibition at Surfaces,
782 The University of Leeds, Leeds.
- 783 Mazzotti, G.M.M.a.M., 2015. Modelling the stochastic behaviour of primary
784 nucleation. *Faraday Discussions*, 179: 359-382.
- 785 Morizot, A.P. and Neville, A., 2000. Barium Sulfate Deposition and Precipitation Using
786 a Combined Electrochemical Surface and Bulk Solution Approach. *Corrosion*,
787 56(06).

- 788 Morizot, A.P. and Neville, A., 2001. Using an Electrochemical Approach for Monitoring
789 Kinetics of CaCO₃ and BaSO₄ Scale Formation and Inhibition on Metal
790 Surfaces. SPE-163105-PA, 6(2): 220-223.
- 791 Morizot, A.P., Neville, A., & Hodgkiess, T., 1999a. Studies of the deposition of CaCO₃
792 on stainless steel surface by a novel electrochemical technique. Journal of
793 Crystal Growth: 198/199, 738/743.
- 794 Myerson, A.S., 2001. Handbook of Industrial Crystallization. Chemical, Petrochemical
795 & Process. Butterworth-Heinemann, 1-304 pp.
- 796 NACE, 2001. Laboratory screening to determine the ability of scale inhibitors to
797 prevent the precipitation of calcium sulfate and calcium carbonate from solution
798 (for oil and gas production systems). NACE Standard Test Method TM 0374
799
- 800 Nielsen, A.E., 1984. Electrolyte crystal growth mechanisms. Journal of Crystal Growth,
801 67(2): 289-310.
- 802 Reddy, M.M. and Hoch, A.R., 2001. Calcite Crystal Growth Rate Inhibition by
803 Polycarboxylic Acids. Journal of Colloid and Interface Science, 235(2): 365-
804 370.
- 805 Sanni, O., Charpentier, T., Kapur, N. and Neville, A., 2015. Study of Surface
806 Deposition and Bulk Scaling Kinetics in Oilfield Conditions Using an In-Situ
807 Flow Rig. In: . (Editor), " Corrosion 2015, 05916 (Dallas, US: NACE, 2015),
808 NACE International, pp. 1-15 pp. 1-15.
- 809 Sanni, O., Charpentier, T., Kapur, N. and Neville, A., 2016. CaCO₃ Scale Surface
810 Nucleation and Growth Kinetics in a Once-Through in situ Flow Rig as a
811 Function of Saturation Ratio (SR), " Corrosion 2016, NACE International. NACE
812 International, Vancouver, Canada, pp. 1-15.
- 813 Sanni, O. et al., 2017. Development of a novel once-through flow visualization
814 technique for kinetic study of bulk and surface scaling. Review of Scientific
815 Instrument, 88(10).
- 816 Seeger, T.S., Muller, E.I., Mesko, M.F. and Duarte, F.A., 2019. Magnesium and
817 calcium determination in desalted crude oil by direct sampling graphite furnace
818 atomic absorption spectrometry. Fuel, 236: 1483-1488.
- 819 Setta, F.A. and Neville, A., 2011. Efficiency assessment of inhibitors on CaCO₃
820 precipitation kinetics in the bulk and deposition on a stainless steel surface
821 (316L). Desalination, 281(1): 340-347.
- 822 Shaw, S. and Sorbie, K., 2013. Structure, Stoichiometry, and Modelling of Calcium
823 Phosphonate Scale Inhibitor Complexes for Application in Precipitation
824 Squeeze Processes, 2013 SPE International Symposium on Oilfield Chemistry.
825 2013, Society of Petroleum Engineers, The Woodlands, TX, USA.
- 826 Shaw, S.S., 2012. Investigation into the mechanism of formation and prevention of
827 Barium sulphate oilfield scale, University of Heriot Watt.
- 828 Tomson, M., et al., 2009. ScaleSoftPitzer Version 4.0, Rice University Brine Chemistry
829 Consortium.
- 830 Tomson, M.B., Kan, A.T. and Fu, G., 2005. Inhibition Of Barite Scale In The Presence
831 Of Hydrate Inhibitors. Society of Petroleum Engineers.

- 832 Yamanaka, S. et al., 2012. Heterogeneous nucleation and growth mechanism on
833 hydrophilic and hydrophobic surface. *Advanced Powder Technology*, 23(2):
834 268-272.
- 835 Yuan, M.D., Jamieson, E. and Hammonds, P., 1998. Investigation of Scaling and
836 Inhibition Mechanisms and the Influencing Factors in Static and Dynamic
837 Inhibition Tests, *CORROSION 98*. NACE International, San Diego, California,
838 pp. 11.
- 839 Zhang, Y., Shaw, H., Farquhar, R. and Dawe, R., 2001. The kinetics of carbonate
840 scaling - Application for the prediction of downhole carbonate scaling. *Journal*
841 *of Petroleum Science and Engineering*, 29(2): 85-95.
- 842